SPANDIDOS
PUBLICATIONS

PGRMC1-dependent autophagy by hyperoside induces apoptosis and sensitizes ovarian cancer cells to cisplatin treatment

XIAOFEI ZHU[1*], MINGDE JI[1*], YUE HAN[2], YUANYUAN GUO[3], WENQIANG ZHU[4],
FENG GAO[1], XUEWEN YANG[1] and CHUNBING ZHANG[1]

Departments of [1]Laboratory Medicine and [2]Gynecology, Affiliated Hospital of Nanjing University of Chinese Medicine,
Nanjing, Jiangsu 210029; [3]Department of Biochemistry, Nanjing University of Chinese Medicine,
Nanjing, Jiangsu 210023; [4]Department of Surgical Oncology, Affiliated Hospital
of Nanjing University of Chinese Medicine, Nanjing, Jiangsu 210029, P.R. China

Abstract. Cisplatin treatment some times leads to chemoresistance, which is now acknowledged partially due to the inductive expression of progesterone receptor membrane component (PGRMC)1 in ovarian cancer cells. PGRMC1 enhances autophagy, activates cytochrome p450, and inveigles signaling pathways to promote cell survival and reduce the effect of drug treatments. In this study, we give first line evidence that hyperoside inhibits cell viability, triggers autophagy and apoptosis in ovarian cancer cell lines. Mechanistically, PGRMC1-dependent autophagy was utilized by hyperoside to induce apoptotic cell death. Hyperoside induced the conversion of LC3B-I to LC3B-II and the formation of autophagosomes in ovarian cancer cells. Notably, PGRMC1 colocolized with LC3B-II, and PGRMC1 overexpression enhanced hyperoside-induced autophagy and apoptosis, while PGRMC1 knockdown abrogated the action. Additionally, AKT signaling and Bcl-2 family were also involved in the hyperoside-induced autophagy and apoptosis. Importantly, in cisplatin-resistant ovarian cancer cells where PGRMC1 was overexpressed, hyperoside sensitized the cells to cisplatin treatment. Together these findings indicate hyperoside functions as a complementary therapy for ovarian cancer patients receiving platinum-based therapy.

Introduction

Ovarian cancer is associated with the highest mortality rate among women of all other gynecological cancers in the world

(1). Surgical removal of the tumor with following platinum-based chemotherapy are the standard methods used to treat the disease (1). However, with increasing chemoresistance level of the tumor, discovery of new effectual alternative approaches is becoming an urgent need.

Flavonoids are a group of the most abundant polyphenols in our daily diet and display a wide range of pharmacological properties (2). Quercetin-3-*O*-β-D-galactopyranoside, also known as hyperoside, is a flavonol glycoside mainly found in plants of the genera *Hypericum* and *Crataegus* (3). Previous studies have shown that hyperoside has anti-oxidant (3,4), anti-inflammatory (5,6) and anticancer activities (7,8). Furthermore, hyperoside produced anticancer effects through inducing apoptosis (8). However, the effect of hyperoside on ovarian cancer cells, especially whether it induces apoptosis, and the underlying mechanisms are all still unknown.

Anticancer drugs induce programmed cell death (PCD). Apoptosis, also known as type I cell death, is regarded as the principal cell death mechanism (9). However, cancer cells trigger multiple pathways to escape from apoptosis (10,11). One of the most important mechanism by which ovarian cancer cells avoid cisplatin-induced apoptosis is that progesterone receptor membrane component (PGRMC) 1 overexpressing in these cells simultaneously induce epithelial grow factor receptor (EGFR) stabilization to promote cell survival and induce cytochrome p450 activation to accelerate drug efflux (12-14). Moreover, the type II PCD, autophagy, which shows a biphasic effect on cell viability, possibly is also responsible for chemoresistance (15). Accordingly, PD168393, an EGFR-TKI, induce autophagy as a cytostatic, but not a cytotoxic, response in malignant peripheral nerve sheath tumor (MPNST) cells that is accompanied by suppression of Akt and mTOR activation (16). In addition to EGFR, genetic and pharmacologic autophagy blockade via PI3K/mTOR inhibition reverses apoptotic resistance and result in significant cell apoptosis (17). Besides, p53 (18), VEGF (19), MAPK14/p38α signaling (20) and microRNAs (21,22) are also engaged in autophagy-mediated cancer cell chemoresistance. Nevertheless, other studies support a role of autophagy for tumor suppression. Patients with low levels of autophagy-related protein (ATG)

Correspondence to: Dr Chunbing Zhang or Dr Xuewen Yang, Department of Laboratory Medicine, Affiliated Hospital of Nanjing University of Chinese Medicine, 155 Hanzhong Road, Nanjing, Jiangsu 210029, P.R. China
E-mail: nju_tcm@163.com
E-mail: firstfisher@163.com

*Contributed equally

5 in their tumors had reduced progression-free survival (23). Ursolic acid promotes cancer cell death by inducing ATG 5-dependent autophagy (24). Thus, molecules leading to cytotoxic autophagy may circumvent apoptotic resistance and benefit cancer treatment.

Notably, a linkage between autophagy and PGRMC1 has been identified (25), PGRMC1 not only induces chemoresistance, but also promotes autophagy. PGRMC1 inhibitor or *PGRMC1*-knockdown leads to autophagic flux inhibition (25). In addition, *PGRMC1*-knockdown cells had increased levels of ubiquitinated proteins, a substrate of autophagy (25). The roles of PGRMC1 and autophagy in the presence of hyperoside in survival of ovarian cancer cells were investigated. We focused on the effect of hyperoside on cell viability, apoptosis and autophagy of ovarian cancer cells, additionally, detailed mechanisms involved including PGRMC1/AKT signaling and Bcl-2 family were thoroughly investigated in this study.

Materials and methods

Cells, plasmids, transfection and reagents. The ovarian cancer cell lines SKOV-3 and HO-8910 were obtained from the American Type Culture Collection (ATCC, Rockville, MD, USA). SKOV-3 and HO-8910 cells were sustained in Dulbecco's modified Eagle's medium (DMEM) (Invitrogen) with 10% (v/v) fetal bovine serum (FBS; Gibco), 100 IU/ml penicillin and 100 ng/ml streptomycin (PAA Laboratories GmbH, Pasching, Austria) at 37˚C, in 5% CO_2 humidified atmosphere. A 603-bp fragment of *PGRMC1* complementary DNA was amplified from SKOV-3 cells by RT-PCR and inserted into the secretory vector, pSecTag2B (a kind gift of Professor C. Lu, Department of Molecular Virology, Nanjing Medical University, China), to generate recombinant pPGRMC1. Short hairpin RNAs for *PGRMC1* knockdown were purchased from Shanghai GenePharma Co. (Shanghai, China) and an optimized shPGRMC1 was determined by western blotting. Transfections of SKOV-3 cells were performed with the Lipofectamine 2000 reagent (Invitrogen Inc., Carlsbad, CA, USA) according to the manufacturer's instructions. Hyperoside (MW: 464.38, HPLC ≥98%), 3-methyladenine (3-MA) and monodansylcadaverine (MDC) were purchased from Sigma-Aldrich Chemical Co. (St. Louis, MO, USA). Hyperoside was dissolved in aqueous DMSO and delivered to cells in media containing this solvent at a final concentration of 0.1% (v/v). Cisplatin was a kind gift of Dr Wei Zhu (26).

Cell proliferation assay. Cell viability in the treated cells was determined by using Cell Counting Kit-8 (CCK-8) kit (Dojindo Laboratories, Kumamoto, Japan) according to the manufacturer's instructions and as previously described by us (27). Briefly, cells were plated at a density of $3x10^3$ cells/well with 100 μl of medium in 96-well plates with increasing doses of hyperoside (0, 50 and 100 μM, dissolved in DMSO). After treatment, CCK-8 solution (10 μl) was added to each well and the plates were incubated at 37˚C for 90 min. The absorbance of the cell suspension was measured with a microplate reader at a wavelength of 490 nm. The highest concentration of hyperoside does not interfere with the CCK-8 assay reagents in the absence of cells (data not shown). Medium containing 10% CCK-8 served as a control.

Plate colony formation assay. To evaluate the ability of cell proliferation, the plate colony formation assay was performed as described previously (28). Briefly, cells ($\sim2x10^2$) were seeded in each well of 12-well plates with complete medium containing hyperoside with increasing concentration from 0 to 100 μM. Cultures were supplemented with conditional complete medium per week. Cells were then fixed in methanol/glacial acetic acid (7:1), washed with water and stained with crystal violet (0.2 g/l). Colonies were scored 14-21 days after seeding the cells.

Cell apoptosis assay. The percentage of cells actively undergoing apoptosis was determined by flow cytometry using an Annexin V assay kit according to the manufacturer's instructions and as previously described (27). Briefly, cells were incubated with increasing doses of hyperoside (vehicle, 50 and 100 μM) for 72 h, and then the cells were harvested with trypsin, washed in phosphate-buffered saline (PBS), and counted. After counting, $1x10^5$ cells were resuspended in binding buffer at a concentration of $1x10^6$ cells/ml. Next, 10 μl of Annexin V and 5 μl of PI were added, and the cells were incubated at room temperature for ≥15 min in the dark. After incubation, the percentage of apoptotic cells was analyzed by flow cytometry (FACScan; BD Biosciences, USA).

Flow cytometry. To detect the expression of LC3B in ovarian cancer cells, $1x10^6$ cells were collected and suspended in cold PBS, fixed with 80% methanol (5 min) and then permeabilized with 0.1% PBS-Tween for 20 min. The cells were then incubated in 1X PBS/10% normal goat serum/0.3 M glycine to block non-specific protein-protein interactions followed by the LC3B mAb (Abcam, ab213934) for 30 min at 22˚C. The secondary antibody used was Alexa Fluor® 488 goat anti-mouse IgG (H+L) (ab150117) at 1:2,000 dilution for 30 min at 22˚C. Acquisition of >10,000 events were collected and analyzed with the FACScan (BD Biosciences).

MDC staining of autophagic vacuoles. MDC staining of autophagic vacuoles was performed for autophagy analysis. Briefly, SKOV-3 cells or HO-8910 cells were seeded onto cover slips placed onto a 6-well plate at a density of $1x10^5$ cells/ml 24 h before treatment and were incubated overnight at 37˚C. After a 48 h treatment with hyperoside (100 μM), the cells were incubated for 20 min with MDC (0.05 mmol/l) at 37˚C and were then washed four times with PBS. Autophagic vacuoles were observed under a fluorescence microscope.

Immunofluorescence staining. For immunofluorescence, cells were fixed in 3:1 methanol:acetone at 4˚C for 45 min as recommended, and then washed, blocked with 10% normal goat serum and probed with mouse anti-LC3B (Abcam, ab213934) and, where indicated, rabbit anti-PGRMC1 (Abcam, ab88381). Fluorescein isothiocyanate (FITC) conjugated goat anti-rabbit IgG (H+L) and Cy3® conjugated goat anti-mouse IgG (H+L) were used as secondary antibodies. All other procedures for staining were according to the manufacturer's instructions. Images were observed and recorded with a Zeiss
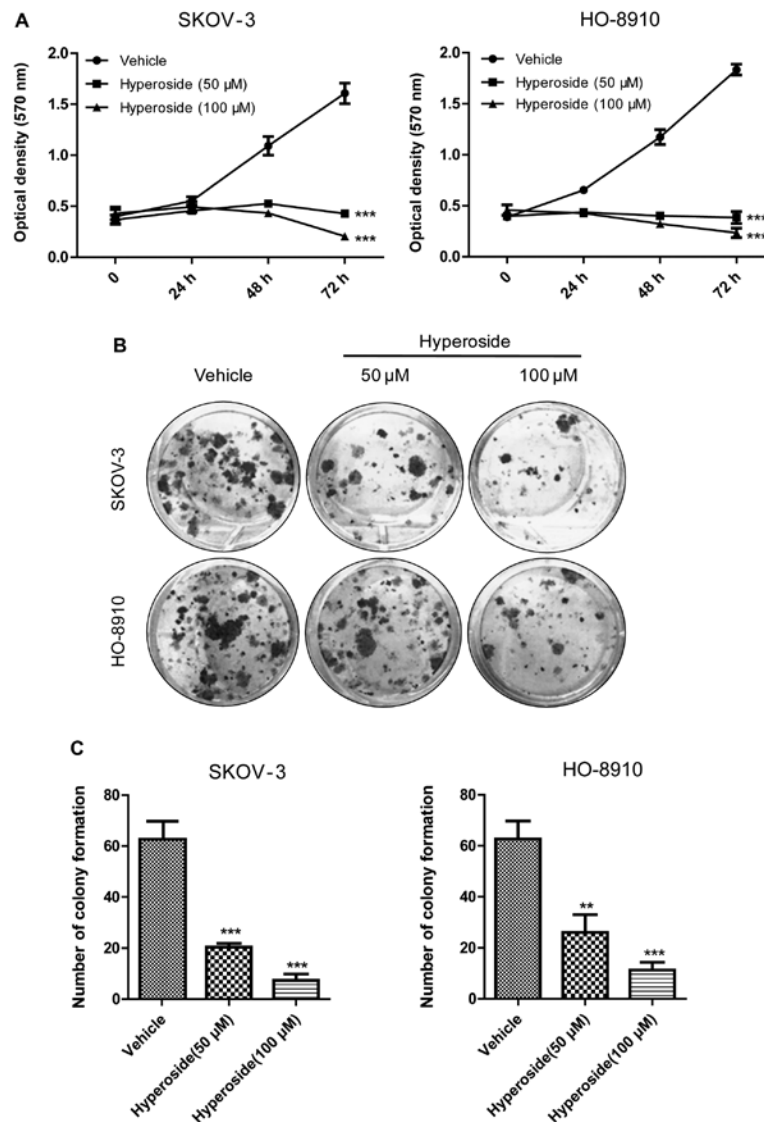
Figure 1. Hyperoside inhibits cell proliferation and colony formation of SKOV-3 and HO-8910 ovarian cancer cell lines. (A) CCK-8 assay of the viability of SKOV-3 or HO-8910 cells treated with vehicle, hyperoside (50 μM) or hyperoside (100 μM) for 24, 48 and 72 h, respectively. ***p<0.001, vs. vehicle-treated cells. (B) Plate colony formation assay for SKOV-3 and HO-8910 cells treated with vehicle, 50 or 100 μM of hyperoside after two weeks. Photographs depict the colony formation. (C) Summary of colony formation numbers in (B). The bars in the graph represent the mean ± SD; shown is one representative experiment of three performed. **p<0.01, and ***p<0.001, vs. vehicle-treated cells.

Axiovert 200 M epifluorescence microscope (Carl Zeiss Inc., Thüringen, Germany).

Western blotting and antibodies. Western blotting was performed as previously described (26,27). Anti-PGRMC1 rabbit polyclonal antibody, and anti-LC3B mouse monoclonal antibody (mAb) were purchased from Abcam Inc. (Abcam, Cambridge, UK). Anti-GAPDH mouse mAb, and horseradish peroxidase (HRP)-conjugated goat anti-mouse and anti-rabbit IgG were purchased from Santa Cruz Biotechnologies (Santa Cruz, CA, USA). Anti-Bcl-2 mouse mAb, anti-Bax rabbit mAb, anti-phospho-AKT (Ser473) mouse mAb, and anti-AKT mouse mAb, were purchased from Cell Signaling Technology (Beverly, MA, USA).

Statistical analysis. Numerical data were expressed as mean ± SD. Two group comparisons were analyzed by two-sided Student's t-test. p-values were calculated, and p<0.05

was considered significant. All experiments were performed at least in triplicate.

Availability of data and materials. Literature collection was performed by using electronic databases PubMed, Cochrane Library, and Web of Science. All statistical analyses were executed by using SPSS 20.0 software (IBM, Chicago, IL, USA). Raw and processed data are stored with the corresponding author of this report and are available upon request.

Results

Effect of hyperoside on viability of ovarian cancer cells. To determine the effect of hyperoside on viability of human ovarian cancer cells, we used SKOV-3 and HO-8910 cells, all of which were exposed to increasing concentrations of hyperoside (0, 50 or 100 μM) for 24, 48 and 72 h. As shown in Fig. 1A hyperoside inhibited the proliferation of both
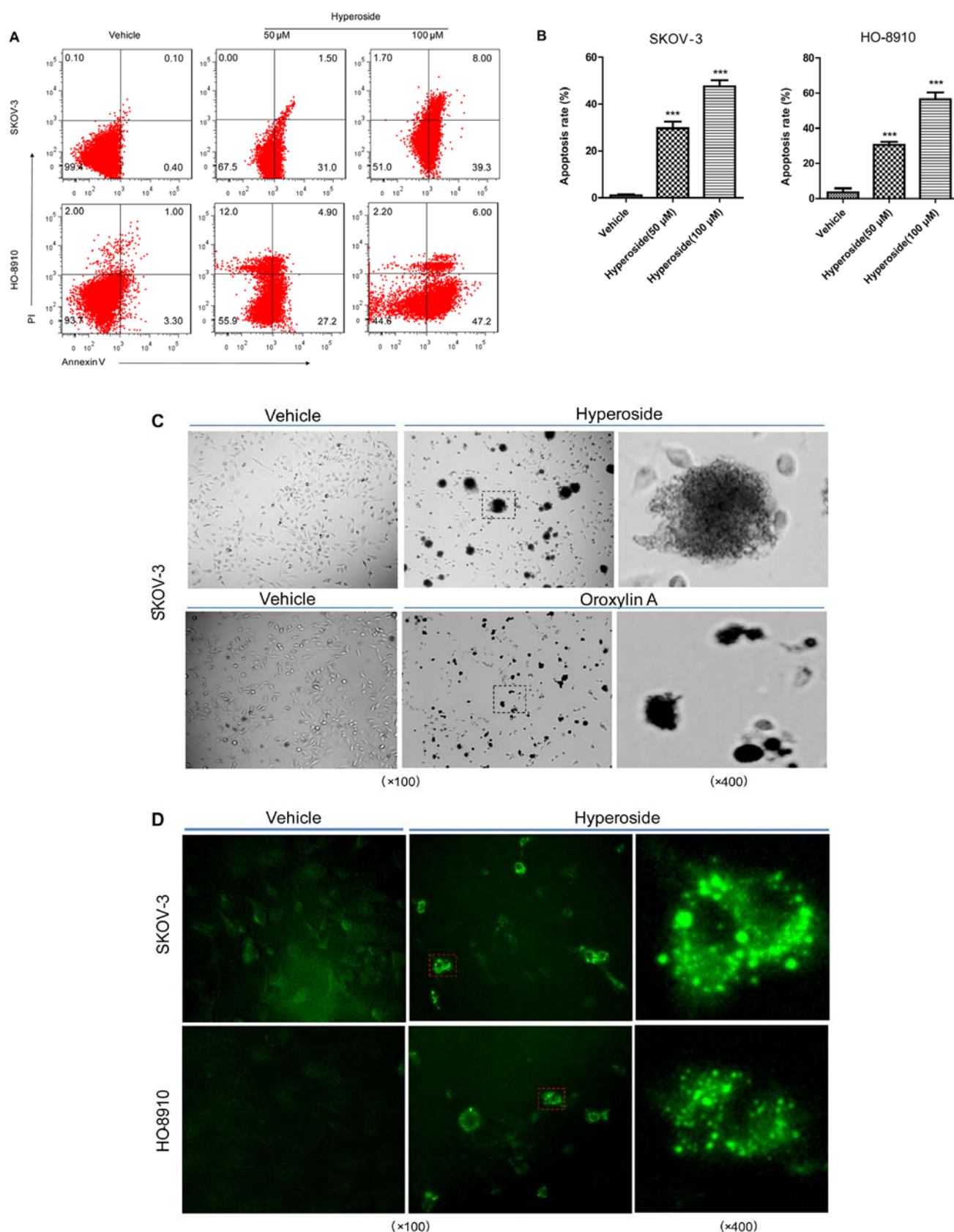
Figure 2. Hyperoside induces apoptosis and autophagy in ovarian cancer cells. (A) Effect of hyperoside on apoptosis of SKOV-3 and HO-8910 cells. SKOV-3 and HO-8910 cells were incubated with hyperoside at 0, 50 and 100 μM. Cells were collected, and apoptotic cells were examined at 48 h post incubtion. x- and y-axes indicated Annexin V and propidium iodide staining intensities, respectively. (B) Summary of percentages of total apoptotic cells in (A), ***p<0.001, vs. vehicle-treated cells. (C) Morphological alteration of SKOV-3 cells upon hyperoside (100 μM) treatment, compared with vehicle- (negative control) or oroxylin A- (disparity control) treated cells. Photographs of hyperoside depict vacuolar structure in SKOV-3 cells (left, original magnification, x100; right, x400). (D) Monodansycadaverine (MDC) staining. SKOV-3 and HO-8910 cells treated with hyperoside (100 μM) for 48 h were incubated with MDC (0.05 mM) for 20 min and observed under a fluorescence microscope (left, original magnification, x100). Inserts are high magnification micrographs of the boxed regions (right, x400).
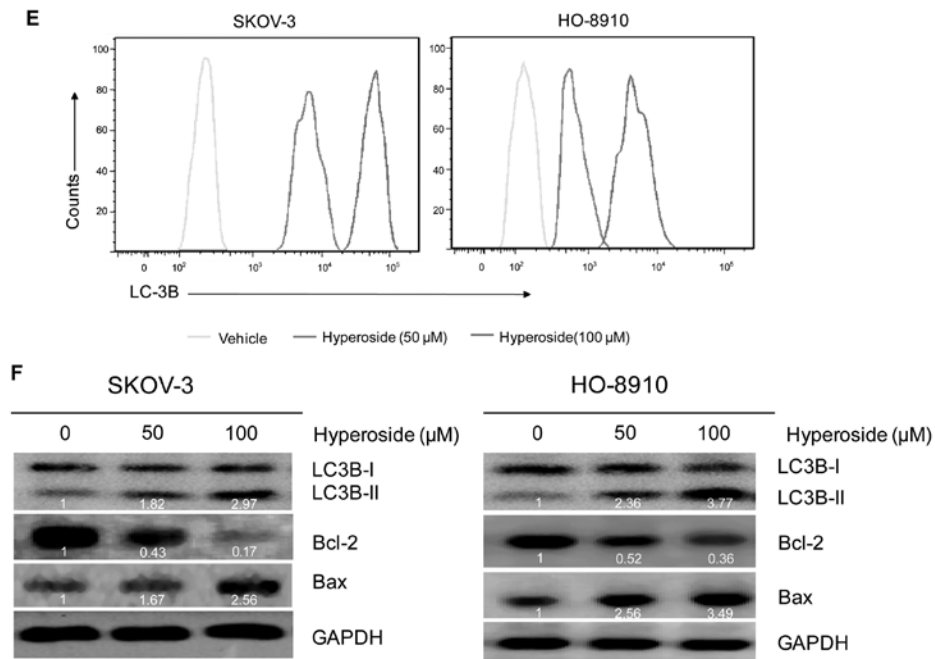
Figure 2. Continued. (E) Representative flow cytometry histograms for LC3B expression in SKOV-3 cells treated as in (A). Cells were stained with anti-LC3B MAb and fluorescein isothiocyanate-labeled IgG was used as secondary antibody. (F) Western blot analysis of LC3B, Bcl-2 and Bax in SKOV-3 and HO-8910 cells incubated with hyperoside at 0, 50 and 100 μM for 48 h. The relative level of LC3B-II, Bcl-2 and Bax were determined by quantitative densitometry compared to GAPDH. The relative value of LC3B-II, Bcl-2 and Bax in vehicle group was considered to be one for comparison, respectively.
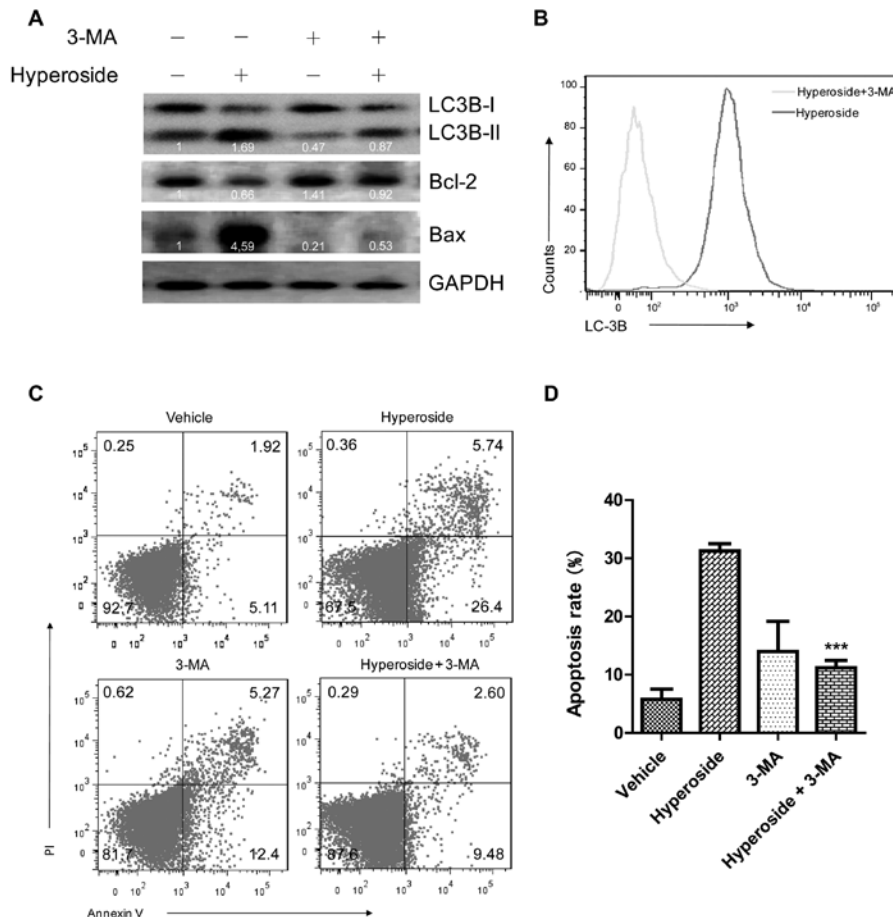

Figure 3. Inhibition of autophagy blocks hyperoside-induced apoptotic cell death. SKOV-3 cells were pretreated with 3-MA (2.5 mM) for 1 h before the addition of hyperoside (100 μM) for another incubation of 48 h. (A) Cellular proteins of the 48-h treatment sample were lysed and subjected to western blot analysis for levels of LC3, Bcl-2 and Bax. The relative value of LC3B-II, Bcl-2 and Bax were determined as mentioned above. (B) Representative flow cytometry histograms for LC3B expression in SKOV-3 cells treated with hyperoside alone or together 3-MA. (C) Cells of the 48-h treatment sample were collected, and apoptotic cells were examined post incubation with Annexin V and propidium iodide, respectively. (D) Summary of percentages of total apoptotic cells in (A).

ovarian cancer cell lines in a dose- and time-dependent manner. Concordantly, in the colony formation assay (Fig. 1B and C), hyperoside suppressed the colony formation of both cancer cells in a dose-dependent manner. Briefly, in SKOV-3 cells, the number of colony formation of 50 or 100 μM group was 20.33±0.88 or 7.33±1.15 respectively, compared with the control group (62.67±6.76). Similarly, in HO-8910 cells, the number of colony formation of 50 or 100 μM group was 26.00±4.04 or 11.33±1.76, compared with the control group (64.88±5.71). Together, these data indicate that hyperoside can effectively inhibit the proliferation of ovarian cancer cells.

Hyperoside induces apoptosis and autophagy in ovarian cancer cells. As hyperoside has a potent anti-proliferative potential in ovarian cancer cells, we suspected that hyperoside induces apoptosis in these tumor cells. Thus, SKOV-3 or HO-8910 cells were treated with various concentrations of hyperoside (0, 50 or 100 μM) for 48 h, stained with Annexin V/ PI, subjected to flow cytometry to determine the apoptosis rate. As we can see in Fig. 2A, the treatment of ovarian cancer cells with various concentrations of hyperoside led to an obvious dose-dependent improvement in both early and late stages of apoptosis. The apoptotic indices were 0.97±0.29, 29.70±1.65, and 47.53±1.59% in SKOV-3 and 3.47±1.31, 30.53±1.03, and 56.50±2.30% in HO-8910 at 0, 50 and 100 μM concentrations of hyperoside, respectively. Additionally, we observed characteristics of vacuolar structure in cancer cells which were exposed to hyperoside, comparing to that of vehicle- or oroxylin A-treated cells (Fig. 2C). Subsequently, as shown in Fig. 2D, the characteristic was validated as autophagic vacuoles by the MDC staining. Considering the linkage between apoptosis and autophagy, we inferred that autophagy may be involved in the hyperoside-induced apoptosis. Then flow cytometry and western blotting were carried out to determine the expression of LC3B, which is a specific marker of autophagy. As shown in Fig. 2E and F, hyperoside dose-dependently increased the level of LC3B in both SKOV-3 (1.82- to 2.97-fold of activation normalized to the control) and HO-8910 (2.36- to 3.77-fold of activation normalized to the control) cells, which indicated that autophagy plays a role at least in part in the hyperoside-induced apoptosis. Concordantly, the expression of Bax/Bcl-2 protein were also in line with the case, where hyperoside treatment downregulated the level of bcl-2 (0.43-0.17 in SKOV-3 or 0.52-0.36 in HO-8910) but increased the expression of bax (1.67-2.56 or 2.56-3.49) in a dose-dependent manner. Together, these results suggest an autophagy-associated cell death by hyperoside in ovarian cancer cells.

Inhibition of autophagy blocks hyperoside-induced apoptotic cell death. Autophagy and apoptosis may act independently in parallel pathways or may influence one another (29). Autophagy may cooperate with apoptosis to promote cell death (30). To test whether hyperoside-induced apoptosis is dependent on autophagy, we investigated the apoptotic effect following autophagy inhibition by 3-MA after hyperoside exposure. SKOV-3 or HO-8910 cells were treated with hyperoside (100 μM) in the presence or absence of 3-MA (2 mM) for 48 h. As shown in Fig. 3A, 3-MA pretreatment significantly decreased the LC3B-II/LC3B-I ratio of hyperoside-treated SKOV-3 cells from 1.69- to 0.87-fold, compared to the cells treated

with hyperoside alone. Similar result was also determined by flow cytometry assay (Fig. 3B). Notably, 3-MA pretreatment markedly attenuated the hyperoside-induced upregulation of Bax (4.59- to 0.53-fold activation) and restored the hyperoside-induced downregulation of Bcl-2 (0.66- to 0.92-fold activation) (Fig. 3A). Finally, assays were carried out to access the effect of 3-MA on cell apoptosis. As expected, SKOV-3 cells with 3-MA pretreatment were restored from hyperoside-induced apoptosis with an apoptotic ratio of 11.21±0.87%, compared to the cells without 3-MA pretreatment of 31.24±0.90%. These results suggest that hyperoside-induced apoptosis of ovarian cancer cells is at least partly dependent on autophagy.

Hyperoside-induced autophagy is dependent on the PGRMC1/AKT pathway. Classical AKT signaling has been shown to be engaged in autophagy (31). Thus, we attempted to find out whether AKT signaling also plays a role in hyperoside-induced autophagy. SKOV-3 cells pretreated with hyperoside (100 μM) for 48 h, were subjected to western blotting. As shown in Fig. 4D, hyperoside inhibited the expression of p-AKT (0.59-fold activation normalized to the control), which suggested that AKT signaling inactivation may be utilized by hyperoside to induce autophagy. PGRMC1 has taken a great part in tumorigenesis by promoting cell invasion and by withstanding drug stress (32). As is the case with autophagy, PGRMC1 promotes recycling substrate to help tumor cells survive (25). However, in the condition of hyperoside, where autophagy is pointing to apoptosis, the effect of PGRMC1 on cell viability and apoptosis is still unclear. Thus, an overexpression construct of PGRMC1 (pPGRMC1) as well as a knockdown shRNAs were transfected into SKOV-3 cells for hyperoside treatment, respectively. Interestingly, PGRMC1 overexpression significantly promoted hyperoside-induced autophagy and cell apoptosis (Fig. 4A-C). Apoptotic ratio of SKOV-3 cells treated with hyperoside plus pPGRMC1 was increased to 32.31±3.30 from 2.50±1.50% of hyperoside alone treated cells. In contrast, when expression of PGRMC1 was knocked down by shRNA, hyperoside-induced autophagy and apoptosis were also abrogated (Fig. 5A-C). Apoptotic ratio of hyperoside plus shPGRMC1-treated SKOV-3 cells was decreased to 6.02±1.28%, compared to that of hyperoside alone treated cells of 19.78±0.72%. Concordantly, at the protein level, PGRMC1 overexpression enhanced LC3B expression in hyperoside-treated SKOV-3 cells (2.77- to 3.21-fold activation) as well as the Bax expression (1.59-1.93), while Bcl-2 expression (0.62-0.34) was decreased (Fig. 4D). Conversely, PGRMC1 knockdown inhibited LC3B (2.69-1.96) and Bax expression (2.33-1.68), while Bcl-2 expression (0.72-1.51) was elevated (Fig. 5D). Also of note is that PGRMC1 alone enhanced phosphorylation of AKT in SKOV-3 cells without hyperoside-treatment (1.71-fold activation), but in the presence of hyperoside, phosphorylation of AKT was reversely exhausted (Fig. 4D). Although the knockdown of PGRMC1 failed to give a significant increase of p-AKT in hyperoside-treated cells (Fig. 5D), PGRMC1/AKT axis at least play a partial role in hyperoside-induced autophagy.

PGRMC1 colocalizes with LC3B to promote hyperoside-induced autophagic cell death and sensitizes ovarian cancer cells to cisplatin treatment. As described in our previous study
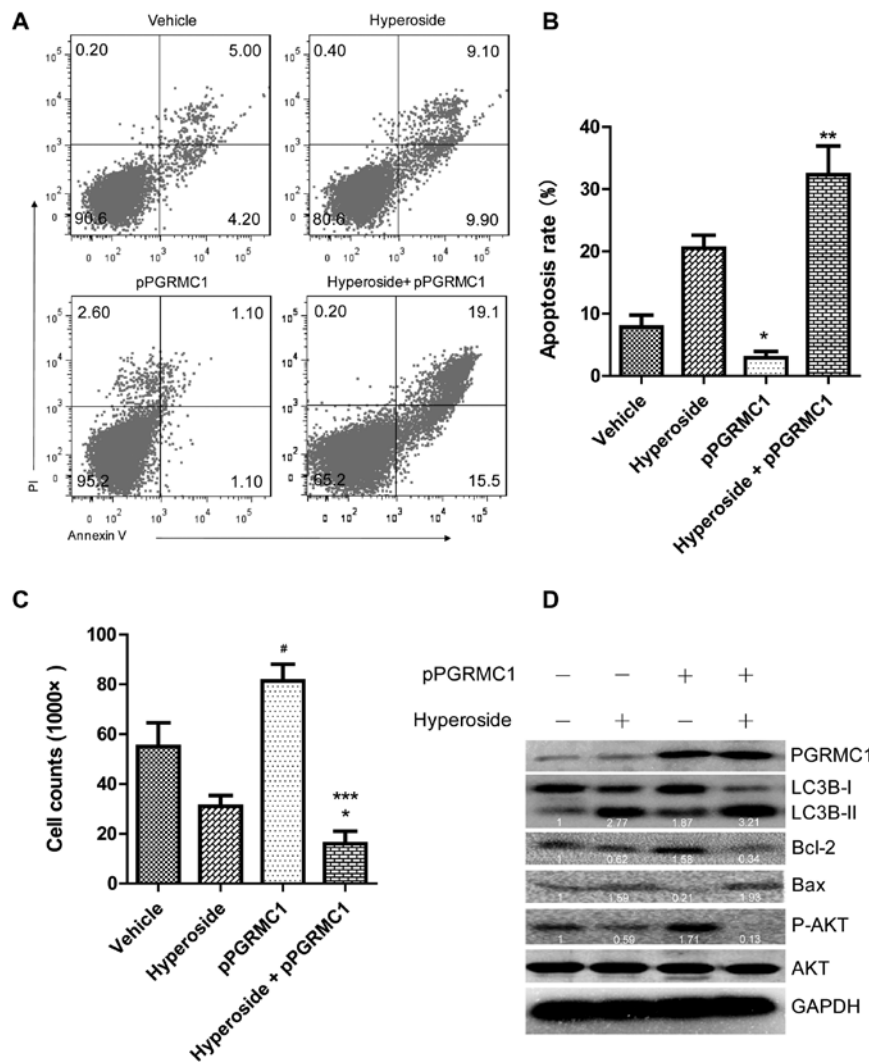
Figure 4. PGRMC1 overexpression induces autophagy and apoptosis in SKOV-3 cells. SKOV-3 cells transfected with or without pPGRMC1 (4 μg) for 24 h were subjected to hyperoside (100 μM) and inculcated for another 24 h. (A) Cells were collected, and incubated with Annexin V and propidium iodide for apoptosis analysis. (B) Summary of percentages of total apoptotic cells in (A), $^*p<0.05$, vs. vehicle-treated cells, $^{***}p<0.001$, vs. hyperoside-treated cells. (C) Cells of the samples were trypsin digested, resuspended in a total volume of 200 μl medium, and cell number was counted by double-blind method. The results represent the mean ± SD; a representative experiment repeated three times is shown. $^*p<0.05$, vs. vehicle-treated cells; and $^{***}p<0.001$, vs. hyperoside-treated cells. (D) Cellular proteins were lysed and subjected to western blot analysis for levels of LC3, Bcl-2, Bax and AKT.

(26), cisplatin-treatment of ovarian cancer would lead to an overexpression of PGRMC1, which then will induce cancer chemoresistance and promote cell survival. However, in this study, we also found a potential of PGRMC1 in promoting hyperoside-induced autophagic cell death. Thus, we inferred that hyperoside may synergistically with cisplatin kill ovarian cancer cells, especially when PGRMC1 is overexpressed. Cell viability and apoptosis of ovarian cancer cells subjected to hyperoside, cisplatin or a combination of both were assessed. As shown in Fig. 6C, cisplatin, at a level of 20 μM, did not significantly inhibit SKOV-3 cell proliferation. However, when in the presence of hyperoside, cisplatin at the same concentration significantly blocked the proliferation of the cells. Moreover, plenty of autophagic vacuoles emerged in cisplatin plus hyperoside treated SKOV-3 cells by the MDC staining, compared to that of cells treated with cisplatin alone (Fig. 6D). In agreement with these findings, cisplatin alone could not induce apparent apoptosis, whereas cisplatin plus hype-

roside induced a large body of apoptosis (Fig. 6A). Notably, co-localization of PGRMC1 with LC-3B in SKOV-3 cells was also determined by immunofluorescence staining as shown in Fig. 6E. Cisplatin alone induced massive expression of PGRMC1, but had no significant effect on LC-3B expression. However, in the presence of hyperoside, abundant PGRMC1 induced by cisplatin co-localized with LC-3B to promote autophagic cell death, thus confirming a striking role of PGRMC1 in hyperoside-induced autophagic cell death. Taken together, in ovarian cancer cells especially the drug-resistant ones where PGRMC1 is overexpressed, hyperoside may utilize this 'Achilles' heel' of PGRMC1 to promote autophagic cell death.

Discussion

Ovarian cancer causes the most mortality in gynecological malignancies (33). However, to date, limited therapeutic
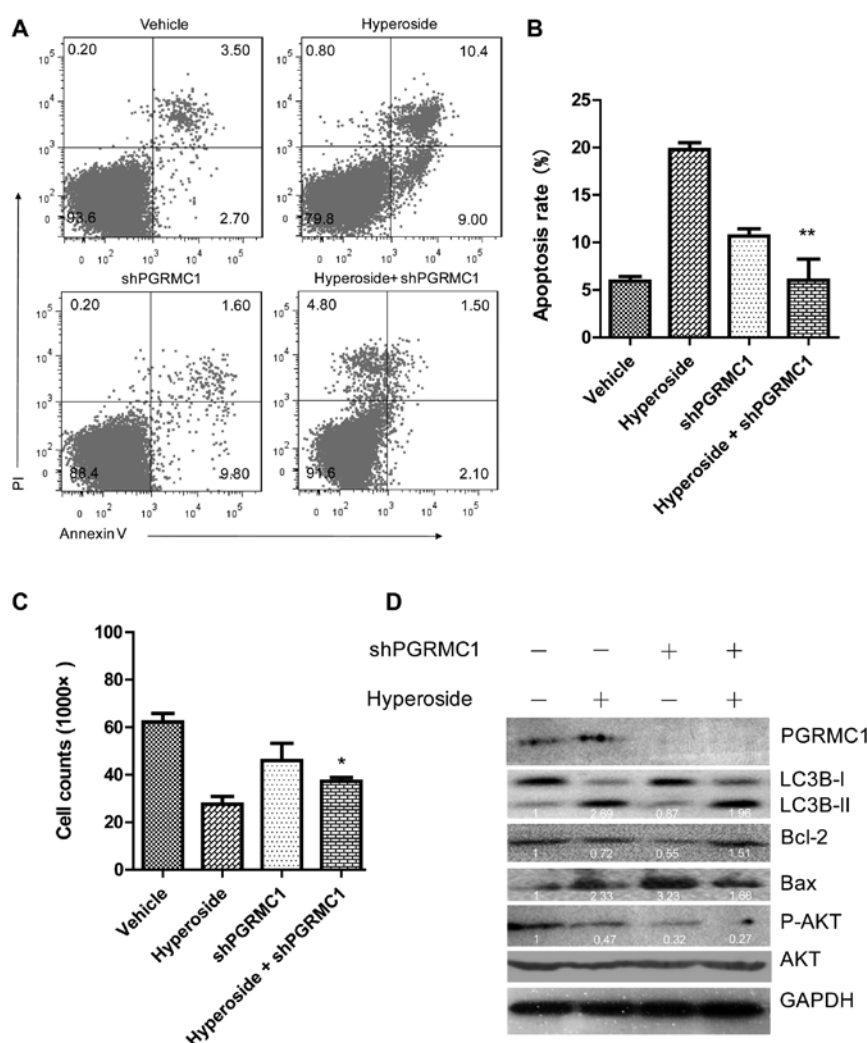
Figure 5. PGRMC1 knockdown inhibits autophagy and apoptosis in SKOV-3 cells. (A) SKOV-3 cells transfected with or without shRNA (4 μg) of *PGRMC1* for 24 h were subjected to hyperoside (100 μM) and inculcated for another 24 h. (A) Cells were collected, and incubated with Annexin V and propidium iodide for apoptosis analysis. (B) Summary of percentages of total apoptotic cells in (A). (C) Cells of the samples were trypsin digested, resuspended in a total volume of 200 μl medium, and cell number was counted by double-blind method. The results represent the mean ± SD; a representative experiment repeated three times is shown. *p<0.05, vs. hyperoside-treated cells. (D) Cellular proteins were lysed and subjected to western blot analysis for levels of LC3, Bcl-2, Bax and AKT.

measures such as surgical resection and platinum-based chemotherapy have shown weak efficacy (33-36). Progesterone receptor membrane component (PGRMC) 1 plays a vital role in the chemoresistance of the cancer. Accordingly, as shown in our previous study, PGRMC1 is elevated in cisplatin-treated HO-8910 cells (26), while also elevated in SKOV-3 cells and ovarian cancer tissues as described by Peluso (37,38). The mechanism by which PGRMC1 mediated chemoresistance is: i) enhancing expression of cytochrome P450 to accelerate drug metabolism (39,40); ii) promoting cancer cell migration and invasion to evade cytotoxicity (38,40,41); and, iii) activating signaling pathways to avoid apoptosis (42). For this reason, ligands targeting PGRMC1 have shown a promising potential in ovarian cancer therapy (43). However, in this study, we first report a feeble effect of the tumor-enhancing protein PGRMC1, which has been utilized by hyperoside to promote autophagy and induce apoptosis in ovarian cancer cells.

In this study, we demonstrated that hyperoside dose-dependently inhibits the proliferation and colony formation of both SKOV-3 and HO-8910 cells. Furthermore, Annexin V/PI double staining showed a dose-dependent apoptotic effect of hyperoside on the cells. This indicated that hyperoside inhibits cell viability by inducing apoptosis. Notably, dose-dependent apoptosis by hyperoside constantly corresponded to a dose-dependent expression of LC3B-II, which suggesting an involvement of autophagy in the hyperoside-mediated apoptosis. Autophagy is an evolutionarily conserved intracellular catabolic process that is used by all cells to degrade dysfunctional or unnecessary cytoplasmic components through delivery to the lysosome (44). However, the role of autophagy in tumor formation is crucial but ambiguous. On one hand, through intracellular recycling, autophagy provides substrates that enable tumor cells to survive the metabolic stress in the tumor microenvironment and promotes tumor progression (44). On the other hand, imbalanced autophagy functions in tumor suppression through directly restricting cell proliferation by inducing cell death (45). To verify the role of autophagy in this case, an autophagy inhibitor, 3-MA was used to block the autophagy by hyperoside. As expected, 3-MA exposure not
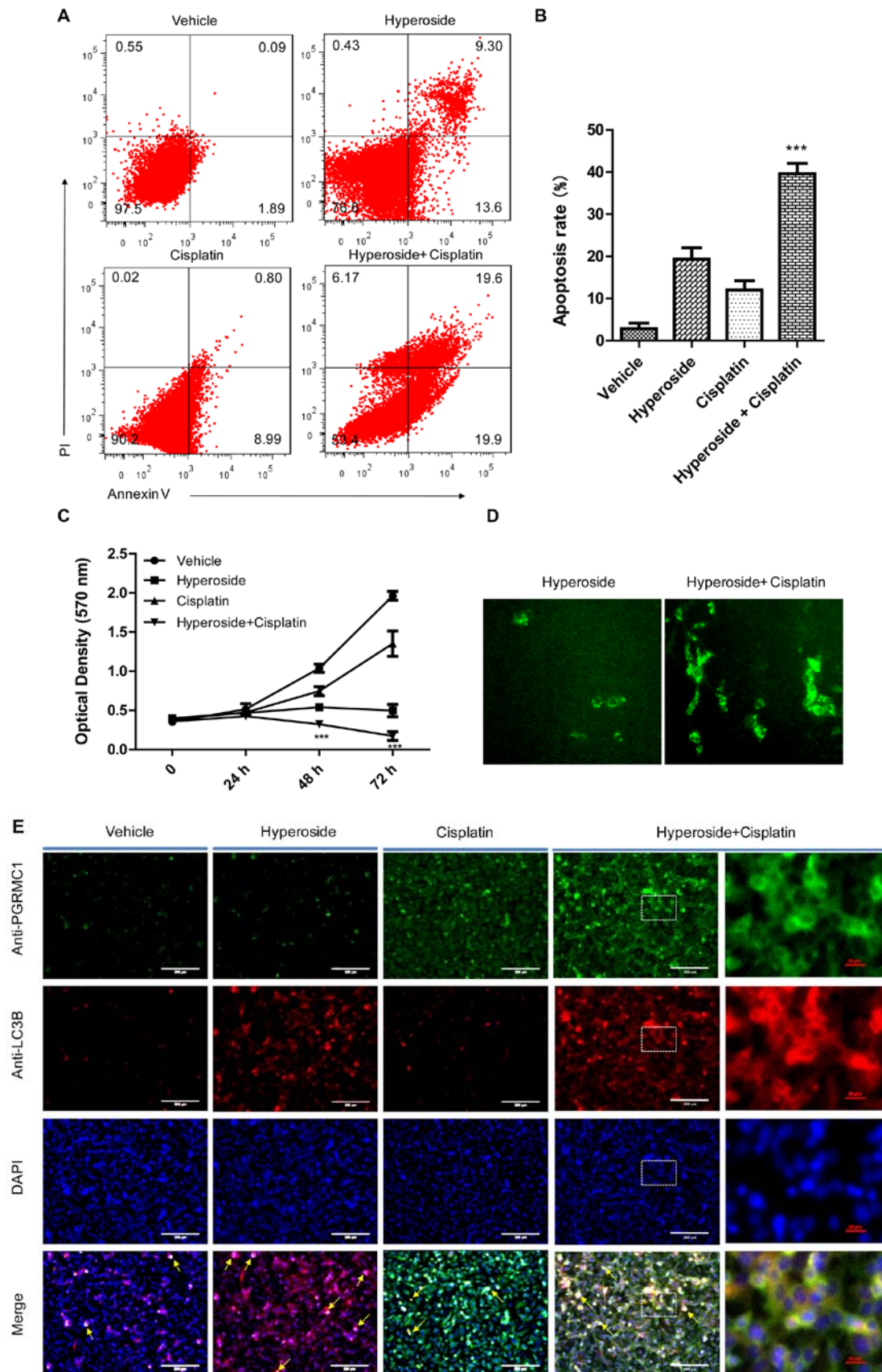
Figure 6. Hyperoside synergizes with cisplatin to promote cell death of SKOV-3 in which LC3B colocalized with PGRMC1. (A) SKOV-3 cells treated with hyperoside (100 μM), cisplatin (20 μM) or hyperoside plus cisplatin were subjected to apoptosis assay. (B) A histogram of percentages of total apoptotic cells is presented with the means ± SE from three independent experiments. ***p<0.001, vs. hyperoside- or cisplatin-treated cells. (C) MTT assay for viability of SKOV-3 cells exposed to hyperoside, cisplatin or hyperoside plus cisplatin, respectively. ***p<0.001 and **p<0.01, vs. cisplatin-treated cells. (D) MDC staining of SKOV-3 cells treated with hyperoside or hyperoside plus cisplatin. Green fluorescence indicates autophagic vacuoles (original magnification, x100). (E) Fluorescence microscopy of SKOV-3 cells incubated for 24 h with hyperoside, cisplatin or hyperoside plus cisplatin, then stained for PGRMC1 (green) and LC3B (red) with rabbit-anti-PGRMC1 and mouse-anti-LC3B antibodies, respectively. FITC-tagged anti-rabbit IgG and CY3-tagged anti-mouse IgG were used as second antibodies. Arrows indicate colocalization of PGRMC1 and LC3B. 4',6'-diamidino-2-phenylindole (DAPI) (blue) stained nuclei.

only gave a reduction in the amount of LC3B protein, but also restored the conversion of LC3B-I to LC3B-II in hyperoside-treated ovarian cancer cells. Autophagy and apoptosis function in parallel tracks but sometimes they also engage in a complex interplay in both physiological and pathological settings (46). Herein, the interplay gave a causal relationship with the fact that autophagy evoked apoptosis in hyperoside-treated ovarian cancer cells. As a result of the autophagy inhibition by 3-MA, the level of Bcl-2 was elevated while the level of Bax was decreased, suggesting a subsequent reversion of apoptosis by 3-MA in hyperoside-treated cancer cells.

Despite these findings, however, the molecular basis of crosstalk is still poorly understood. AKT signaling is now acknowledged to be the crucial pathway which manipulates the autophagy processing (31,47). Given a linkage between AKT signaling and PGRMC1/2 family by our previous study (26), we inferred that PGRMC1/2 family may also take part in the hyperoside-mediated autophagy and apoptosis. In fact, Mir and colleagues identified an association between PGRMC1 and LC3B in A549 cells where PGRMC1 shows cytoprotective effects (25). The role of PGRMC1 in hyperoside-induced autophagy and apoptosis was explored. Regarding an elevation of PGRMC1 by cisplatin in ovarian cancer cells, we suspected hyperoside induced-autophagy was the result of an alteration of the PGRMC1 expression. However, treatment of hyperoside from 0 to 100 μM did not alter the expression profile of PGRMC1 (data not shown). We attempted to clarify the role of PGRMC1 in hyperoside-mediated autophagy and apoptosis. A recombinant PGRMC1 overexpressing plasmid was transfected into the SKOV-3 cells. Our results are in line with the findings by Mir *et al* (25) that PGRMC1 overexpression enhanced autophagic flux while it was inhibited upon PGRMC1 knockdown. However, beyond our expectations and as contradiction to the notions of PGRMC1 having tumor-promoting capacity, in the presence of hyperoside, overexpression of PGRMC1 led to cell death of ovarian cancer. Simultaneously, PGRMC1 overexpression in SKOV-3 cells with hyperoside exposure elevated the level of LC3B-II, a conversion from LC3B-I constantly indicates a formation of autophagosomes. Concordantly, PGRMC1 knockdown by specific shRNA significantly abrogated hyperoside-induced autophagic cell death and decreased LC3B-II values. All these results indicate a tumor-inhibiting instead of tumor-promoting effect of PGRMC1 in hyperoside-treated ovarian cancer cells.

Crosstalk between the apoptotic and autophagic machineries is emerging as a recurring theme with particular importance for Bcl-2 family proteins in bridging the two pathways (48). In the present study, Bcl-2 family had also taken part in the PGRMC1-dependent autophagy and apoptosis by hyperoside. Indeed, ectopic PGRMC1 elevated Bcl-2 expression and dropped Bax expression, yet, in the presence of hyperoside, ectopic PGRMC1 reversed the expression profile of the proteins by dropping Bcl-2 and increasing Bax. The role of Bcl-2 family in relation to autophagy and apoptosis is complicated and is still unclear, but in this study, we showed experimental evidence that Bcl-2 family plays a role at least in part in the hyperoside-induced autophagy and apoptosis.

Autophagy shows either cytoprotective or cytotoxic effect on cell fate depending on the context. In this study, in the presence of hyperoside, extremely imbalanced autophagic flux

led to cytotoxic effect on ovarian cancer cells. In particular, PGRMC1 colocalized with LC3B to promote autophagy and apoptosis. LC3 (or MAP1LC3) is an ubiquitin like ortholog of yeast Atg8 (49), which is required for autophagy (50). Accordingly, PGRMC1 binds to LC3B-II and is essential for the degradative activity of autophagy (25). PGRMC1 engages in the fusion of autophagosomes with lysosomes (51), which in turn activate mitochondrial apoptosis (52,53). Thus, the tumor-inhibiting effect of PGRMC1 by hyperoside given in this study may ascribe to the combination of these two molecules that collaboratively triggered imbalanced autophagic flux and led to subsequent apoptotic cell death.

Pathophysiologically and coincidentally, *in vitro* and *in vivo* cisplatin treatment lead to PGRMC1 overexpression in ovarian cancer cells. Thus, utilization of the 'Achilles' heel' of PGRMC1 which functions as autophagy-enhancing and tumor-inhibiting effect by hyperoside may benefit and highlight a possible cure of the ovarian cancer patients.

In conclusion, in this study, we explored the effectiveness of hyperoside on treatment of ovarian cancer cells. Mechanistically, a central role of PGRMC1 played in the action was determined. We found that PGRMC1 colocalized with LC3B to participate in the autophagy and apoptosis by hyperoside. PGRMC1 overexpression significantly promoted hyperoside-induced autophagy and apoptosis, while PGRMC1 knockdown abrogated the action. Additionally, in ovarian cancer cells where PGRMC1 is overexpressed, hyperoside enhanced sensitivity of cells to cisplatin treatment. Although we found the involvement of Bcl-2 family in the hyperoside-mediated autophagy and apoptosis, the exact role of the family particularly in bridging autophagy and apoptosis processes should be further investigated.

References

1. Salzberg M, Thurlimann B, Bonnefois H, Fink D, Rochlitz C, von Moos R and Senn H: Current concepts of treatment strategies in advanced or recurrent ovarian cancer. Oncology 68: 293-298, 2005.
2. Middleton E Jr, Kandaswami C and Theoharides TC: The effects of plant flavonoids on mammalian cells: Implications for inflammation, heart disease, and cancer. Pharmacol Rev 52: 673-751, 2000.
3. Zou Y, Lu Y and Wei D: Antioxidant activity of a flavonoid-rich extract of *Hypericum perforatum* L. in vitro. J Agric Food Chem 52: 5032-5039, 2004.
4. Piao MJ, Kang KA, Zhang R, Ko DO, Wang ZH, You HJ, Kim HS, Kim JS, Kang SS and Hyun JW: Hyperoside prevents oxidative damage induced by hydrogen peroxide in lung fibroblast cells via an antioxidant effect. Biochim Biophys Acta 1780: 1448-1457, 2008.
5. Ku SK, Zhou W, Lee W, Han MS, Na M and Bae JS: Anti-inflammatory effects of hyperoside in human endothelial cells and in mice. Inflammation 38: 784-799, 2015.
6. Ku SK, Kwak S, Kwon OJ and Bae JS: Hyperoside inhibits high-glucose-induced vascular inflammation in vitro and in vivo. Inflammation 37: 1389-1400, 2014.

7. Lü P: Inhibitory effects of hyperoside on lung cancer by inducing apoptosis and suppressing inflammatory response via caspase-3 and NF-κB signaling pathway. Biomed Pharmacother 82: 216-225, 2016.

8. Boukes GJ and van de Venter M: The apoptotic and autophagic properties of two natural occurring prodrugs, hyperoside and hypoxoside, against pancreatic cancer cell lines. Biomed Pharmacother 83: 617-626, 2016.

9. Yuan J and Horvitz HR: A first insight into the molecular mechanisms of apoptosis. Cell 116: S53-S56, 51 p following S59, 2004.

10. Yaacoub K, Pedeux R, Tarte K and Guillaudeux T: Role of the tumor microenvironment in regulating apoptosis and cancer progression. Cancer Lett 378: 150-159, 2016.

11. Ivanov VN, Bhoumik A and Ronai Z: Death receptors and melanoma resistance to apoptosis. Oncogene 22: 3152-3161, 2003.

12. Ahmed IS, Rohe HJ, Twist KE and Craven RJ: PGRMC1 (progesterone receptor membrane component 1) associates with epidermal growth factor receptor and regulates erlotinib sensitivity. J Biol Chem 285: 24775-24782, 2010.

13. Kabe Y, Nakane T, Koike I, Yamamoto T, Sugiura Y, Harada E, Sugase K, Shimamura T, Ohmura M, Muraoka K, et al: Haem-dependent dimerization of PGRMC1/Sigma-2 receptor facilitates cancer proliferation and chemoresistance. Nat Commun 7: 11030, 2016.

14. Szczesna-Skorupa E and Kemper B: Progesterone receptor membrane component 1 inhibits the activity of drug-metabolizing cytochromes P450 and binds to cytochrome P450 reductase. Mol Pharmacol 79: 340-350, 2011.

15. Zheng K, Li Y, Wang S, Wang X, Liao C, Hu X, Fan L, Kang Q, Zeng Y, Wu X, et al: Inhibition of autophagosome-lysosome fusion by ginsenoside Ro via the ESR2-NCF1-ROS pathway sensitizes esophageal cancer cells to 5-fluorouracil-induced cell death via the CHEK1-mediated DNA damage checkpoint. Autophagy 12: 1593-1613, 2016.

16. Kohli L, Kaza N, Lavalley NJ, Turner KL, Byer S, Carroll SL and Roth KA: The pan erbB inhibitor PD168393 enhances lysosomal dysfunction-induced apoptotic death in malignant peripheral nerve sheath tumor cells. Neuro-oncol 14: 266-277, 2012.

17. Ghadimi MP, Lopez G, Torres KE, Belousov R, Young ED, Liu J, Brewer KJ, Hoffman A, Lusby K, Lazar AJ, et al: Targeting the PI3K/mTOR axis, alone and in combination with autophagy blockade, for the treatment of malignant peripheral nerve sheath tumors. Mol Cancer Ther 11: 1758-1769, 2012.

18. Amaravadi RK, Yu D, Lum JJ, Bui T, Christophorou MA, Evan GI, Thomas-Tikhonenko A and Thompson CB: Autophagy inhibition enhances therapy-induced apoptosis in a Myc-induced model of lymphoma. J Clin Invest 117: 326-336, 2007.

19. Stanton MJ, Dutta S, Zhang H, Polavaram NS, Leontovich AA, Hönscheid P, Sinicrope FA, Tindall DJ, Muders MH and Datta K: Autophagy control by the VEGF-C/NRP-2 axis in cancer and its implication for treatment resistance. Cancer Res 73: 160-171, 2013.

20. de la Cruz-Morcillo MA, Valero ML, Callejas-Valera JL, Arias-González L, Melgar-Rojas P, Galán-Moya EM, García-Gil E, García-Cano J and Sánchez-Prieto R: P38MAPK is a major determinant of the balance between apoptosis and autophagy triggered by 5-fluorouracil: Implication in resistance. Oncogene 31: 1073-1085, 2012.

21. Weidhaas JB, Babar I, Nallur SM, Trang P, Roush S, Boehm M, Gillespie E and Slack FJ: MicroRNAs as potential agents to alter resistance to cytotoxic anticancer therapy. Cancer Res 67: 11111-11116, 2007.

22. Yu Y, Cao L, Yang L, Kang R, Lotze M and Tang D: microRNA 30A promotes autophagy in response to cancer therapy. Autophagy 8: 853-855, 2012.

23. Liu H, He Z, von Rütte T, Yousefi S, Hunger RE and Simon HU: Down-regulation of autophagy-related protein 5 (ATG5) contributes to the pathogenesis of early-stage cutaneous melanoma. Sci Transl Med 5: 202ra123, 2013.

24. Leng S, Hao Y, Du D, Xie S, Hong L, Gu H, Zhu X, Zhang J, Fan D and Kung HF: Ursolic acid promotes cancer cell death by inducing Atg5-dependent autophagy. Int J Cancer 133: 2781-2790, 2013.

25. Mir SU, Schwarze SR, Jin L, Zhang J, Friend W, Miriyala S, St Clair D and Craven RJ: Progesterone receptor membrane component 1/Sigma-2 receptor associates with MAP1LC3B and promotes autophagy. Autophagy 9: 1566-1578, 2013.

26. Zhu X, Han Y, Fang Z, Wu W, Ji M, Teng F, Zhu W, Yang X, Jia X and Zhang C: Progesterone protects ovarian cancer cells from cisplatin-induced inhibitory effects through progesterone receptor membrane component 1/2 as well as AKT signaling. Oncol Rep 30: 2488-2494, 2013.

27. Zhu X, Guo Y, Yao S, Yan Q, Xue M, Hao T, Zhou F, Zhu J, Qin D and Lu C: Synergy between Kaposi's sarcoma-associated herpesvirus (KSHV) vIL-6 and HIV-1 Nef protein in promotion of angiogenesis and oncogenesis: Role of the AKT signaling pathway. Oncogene 33: 1986-1996, 2014.

28. Xue M, Yao S, Hu M, Li W, Hao T, Zhou F, Zhu X, Lu H, Qin D, Yan Q, et al: HIV-1 Nef and KSHV oncogene K1 synergistically promote angiogenesis by inducing cellular miR-718 to regulate the PTEN/AKT/mTOR signaling pathway. Nucleic Acids Res 42: 9862-9879, 2014.

29. Zhu H and Zhang Y: Life and death partners in post-PCI restenosis: Apoptosis, autophagy, and the cross-talk between them. Curr Drug Targets: Jun 24, 2016 (Epub ahead of print).

30. Dalby KN, Tekedereli I, Lopez-Berestein G and Ozpolat B: Targeting the prodeath and prosurvival functions of autophagy as novel therapeutic strategies in cancer. Autophagy 6: 322-329, 2010.

31. Wang RC, Wei Y, An Z, Zou Z, Xiao G, Bhagat G, White M, Reichelt J and Levine B: Akt-mediated regulation of autophagy and tumorigenesis through Beclin 1 phosphorylation. Science 338: 956-959, 2012.

32. Cahill MA, Jazayeri JA, Catalano SM, Toyokuni S, Kovacevic Z and Richardson DR: The emerging role of progesterone receptor membrane component 1 (PGRMC1) in cancer biology. Biochim Biophys Acta 1866: 339-349, 2016.

33. Grabowski JP and Sehouli J: Current management of ovarian cancer. Minerva Med 106: 151-156, 2015.

34. Herzog TJ: The current treatment of recurrent ovarian cancer. Curr Oncol Rep 8: 448-454, 2006.

35. Absolom K, Eiser C, Turner L, Ledger W, Ross R, Davies H, Coleman R, Hancock B, Snowden J and Greenfield D; Late Effects Group Sheffield: Ovarian failure following cancer treatment: Current management and quality of life. Hum Reprod 23: 2506-2512, 2008.

36. Rodriguez-Freixinos V, Mackay HJ, Karakasis K and Oza AM: Current and emerging treatment options in the management of advanced ovarian cancer. Expert Opin Pharmacother 17: 1063-1076, 2016.

37. Peluso JJ: Non-genomic actions of progesterone in the normal and neoplastic mammalian ovary. Semin Reprod Med 25: 198-207, 2007.

38. Peluso JJ: Progesterone signaling mediated through progesterone receptor membrane component-1 in ovarian cells with special emphasis on ovarian cancer. Steroids 76: 903-909, 2011.

39. Oda S, Nakajima M, Toyoda Y, Fukami T and Yokoi T: Progesterone receptor membrane component 1 modulates human cytochrome p450 activities in an isoform-dependent manner. Drug Metab Dispos 39: 2057-2065, 2011.

40. Albrecht C, Huck V, Wehling M and Wendler A: In vitro inhibition of SKOV-3 cell migration as a distinctive feature of progesterone receptor membrane component type 2 versus type 1. Steroids 77: 1543-1550, 2012.

41. Ahmed IS, Rohe HJ, Twist KE, Mattingly MN and Craven RJ: Progesterone receptor membrane component 1 (Pgrmc1): A heme-1 domain protein that promotes tumorigenesis and is inhibited by a small molecule. J Pharmacol Exp Ther 333: 564-573, 2010.

42. Peluso JJ, Liu X, Gawkowska A, Lodde V and Wu CA: Progesterone inhibits apoptosis in part by PGRMC1-regulated gene expression. Mol Cell Endocrinol 320: 153-161, 2010.

43. van Waarde A, Rybczynska AA, Ramakrishnan NK, Ishiwata K, Elsinga PH and Dierckx RA: Potential applications for sigma receptor ligands in cancer diagnosis and therapy. Biochim Biophys Acta 1848B: 2703-2714, 2015.

44. Lin L and Baehrecke EH: Autophagy, cell death, and cancer. Mol Cell Oncol 2: e985913, 2015.

45. Gewirtz DA: Cytoprotective and nonprotective autophagy in cancer therapy. Autophagy 9: 1263-1265, 2013.

46. Eisenberg-Lerner A, Bialik S, Simon HU and Kimchi A: Life and death partners: Apoptosis, autophagy and the cross-talk between them. Cell Death Differ 16: 966-975, 2009.

47. Petiot A, Ogier-Denis E, Blommaart EF, Meijer AJ and Codogno P: Distinct classes of phosphatidylinositol 3'-kinases are involved in signaling pathways that control macroautophagy in HT-29 cells. J Biol Chem 275: 992-998, 2000.

48. Rubinstein AD, Eisenstein M, Ber Y, Bialik S and Kimchi A: The autophagy protein Atg12 associates with antiapoptotic Bcl-2 family members to promote mitochondrial apoptosis. Mol Cell 44: 698-709, 2011.
49. Mann SS and Hammarback JA: Molecular characterization of light chain 3. A microtubule binding subunit of MAP1A and MAP1B. J Biol Chem 269: 11492-11497, 1994.
50. Tsukada M and Ohsumi Y: Isolation and characterization of autophagy-defective mutants of *Saccharomyces cerevisiae*. FEBS Lett 333: 169-174, 1993.
51. Ostenfeld MS, Høyer-Hansen M, Bastholm L, Fehrenbacher N, Olsen OD, Groth-Pedersen L, Puustinen P, Kirkegaard-Sørensen T, Nylandsted J, Farkas T, *et al*: Anti-cancer agent siramesine is a lysosomotropic detergent that induces cytoprotec- tive autophagosome accumulation. Autophagy 4: 487-499, 2008.
52. Ishisaka R, Kanno T, Akiyama J, Yoshioka T, Utsumi K and Utsumi T: Activation of caspase-3 by lysosomal cysteine proteases and its role in 2,2'-azobis- (2-amidinopropane)dihydro- chloride (AAPH)-induced apoptosis in HL-60 cells. J Biochem 129: 35-41, 2001.
53. Stoka V, Turk B, Schendel SL, Kim TH, Cirman T, Snipas SJ, Ellerby LM, Bredesen D, Freeze H, Abrahamson M, *et al*: Lysosomal protease pathways to apoptosis. Cleavage of bid, not pro-caspases, is the most likely route. J Biol Chem 276: 3149-3157, 2001.